Develop. Growth Differ. (2008) **50**, 189–201 doi: 10.1111/j.1440-169x.2008.00988.x

Mitochondrial behavior during oogenesis in zebrafish: A confocal microscopy analysis

Yong-Zhong Zhang,[1,2] Ying-Chun Ouyang,[1] Yi Hou,[1] Heide Schatten,[3] Da-Yuan Chen[1] and Qing-Yuan Sun[1,*]

[1]*State Key Laboratory of Reproductive Biology, Institute of Zoology, Chinese Academy of Sciences, Datun Road, Chaoyang, Beijing 100101,* [2]*Department of Life Sciences, Liaocheng University, Liaocheng, China; and* [3]*Department of Veterinary Pathobiology, School of Veterinary Medicine, University of Missouri-Columbia, Columbia, Missouri, USA*

The behavior of mitochondria during early oogenesis remains largely unknown in zebrafish. We used three mitochondrial probes (Mito Tracker Red CMXRos, Mito Tracker Green FM, and JC-1) to stain early zebrafish oocyte mitochondria, and confocal microscopy to analyze mitochondrial aggregation and distribution. By using fluorescence recovery after photobleaching (FRAP), we traced mitochondrial movement. The microtubule assembly inhibitor nocodazole and microfilament inhibitor cytochalasin B (CB) were used to analyze the role of microtubules and microfilaments on mitochondrial movement. By using the dual emission probe, JC-1, and oxidative phosphorylation uncoupler, carbonyl cyanide 4-(trifluoromethoxy) phenylhydrazone (FCCP), we determined the distribution of active and inactive (low-active) mitochondria. Green/red fluorescence ratios of different sublocations in different oocyte groups stained by JC-1 were detected in merged (green and red) images. Our results showed that mitochondria exhibited a unique distribution pattern in early zebrafish oocytes. They tended to aggregate into large clusters in early stage I oocytes, but in a threadlike state in latter stage I oocytes. We detected a lower density mitochondrial area and a higher density mitochondrial area on opposite sides of the germinal vesicle. The green/red fluorescence ratios in different sublocations in normal oocytes were about 1:1. This implies that active mitochondria were distributed in all sublocations. FCCP treatment caused significant increases in the ratios. CB and nocodazole treatment caused an increase of the ratios in clusters and mitochondrial cloud, but not in dispersed areas. Mitochondria in different sublocations underwent fast dynamic movement. Inhibition or disruption of microtubules or microfilaments resulted in even faster mitochondrial free movement.

Key words: confocal, mitochondrion, oocyte, oogenesis, zebrafish.

Introduction

Mitochondria are generally known as the powerhouses of eukaryotic cells because of their major role in oxidative phosphorylation and ATP production, but they carry out various other important functions and contribute to redox and Ca^{2+} homeostasis, provide intermediary metabolites, store pro-apoptotic factors, and organize and transport germ plasm during animal oogenesis. The mitochondrial genome in animal cells has been conserved throughout evolution for more than half a billion years; all mitochondrial DNA (mtDNA) in metazoic cells have a similar length from 13 to 19 kbp, containing 37 genes. Mitochondrial genes have no intron, and have little if any intervals between genes, except for the regulating un-coding region of the D-loop (Reynier *et al*. 1998; Saccone *et al*. 2002; Pakendorf & Stoneking 2005; Cao *et al*. 2007; Webster *et al*. 2007). The mitochondrial genome is vulnerable to fast accumulation of deleterious mutations during an individual animal's life time (Wallace *et al*. 1988; Suganuma *et al*. 1993; Wallace *et al*. 1995). Mitochondria in animal oocytes actively participate in germ plasm formation and translocation; mitochondria in the germ plasm are highly active (Wilding *et al*. 2001b), although their exact role in germ plasm processes remains unclear. Several investigators proposed a bottleneck hypothesis to explain the strict limitation of deleterious mutations in the mitochondrial genome (Bergstrom & Pritchard 1998; Jansen & de Boer 1998; Marchington *et al*. 1998), but it could not be explained why obvious positive or neutral mutation (except for point mutations within genes) did not occur in mtDNAs

*Author to whom all correspondence should be addressed.
Email: sunqy@ioz.ac.cn
Received 20 October 2007; revised 14 November 2007; accepted 17 December 2007.

during the 800 million years of animal evolution (Saccone *et al*. 2002). There may be mechanisms other than the proposed bottleneck that exist in one or more periods of animal oogenesis to preserve the integrity of the mitochondrial genome, since sperm do not transmit their mitochondria to offspring under normal conditions. The close relationship of mitochondria with germ plasm during early oogenesis may be related to preservation of mitochondrial genome integrity.

During oogenesis of many animals, including *Drosophila*, zebrafish, *Xenopus*, mouse, pig, and human, mitochondria undergo a series of changes in their morphology, quantity, subcellular localization, and aggregation (Barritt *et al*. 1999; Perez *et al*. 2000; Sun *et al*. 2001; Wilding *et al*. 2001a; Barritt *et al*. 2002; Van Blerkom *et al*. 2002; Nishi *et al*. 2003; Torner *et al*. 2004; Cao *et al*. 2007; Dumollard *et al*. 2007). The close relationship between mitochondria and germ plasm during oogenesis has been reported in many vertebrates (Kloc & Etkin 1998; Knaut *et al*. 2000; Reunov *et al*. 2000; Kosaka *et al*. 2007). Large and small mitochondrial rRNAs (mtlrRNA and mtsrRNA) have been found outside mitochondria in the germ plasm of *Drosophila* (Kobayashi & Okada 1989; Ding *et al*. 1993; Kobayashi *et al*. 1993; Iida & Kobayashi 1998; Amikura *et al*. 2001, 2005) and *Xenopus* (Kobayashi *et al*. 1998; Kashikawa *et al*. 2001). These mitochondrial rRNAs together with mitochondrial ribosomal proteins form mitochondrial ribosomes translate protein in germ plasm outside the mitochondrion (Amikura *et al*. 2001, 2005). It was also demonstrated that injection of mitochondrial rRNA into ultraviolet-irradiated *Drosophila* embryos restored the pole cell-forming ability (Kobayashi & Okada 1989).

In *Xenopus* and zebrafish, it has been reported that from the late oogonia stage to early stage I oocytes, the germ plasm, including the germ line determining RNAs, such as Xlsirts, Xwnt-11, and Xcat2, move out of the nucleus and become intimately associated with mitochondria. Together they form the mitochondrial cloud (MC) (Kloc *et al*. 1993; Kloc & Etkin 1994, 1995, 1998; Forristall *et al*. 1995; Biliński *et al*. 2004; Kosaka *et al*. 2007). The MC, along with the germ plasm gradually moves from the perinuclear area to the vegetal cortex during early oogenesis. This process is microtubule- and microfilament-independent (Kloc & Etkin 1995; Kloc *et al*. 1996), which is different from other cellular systems in which mitochondria translocation typically depends on microtubules (Karbowski *et al*. 2000; Sun *et al*. 2001; Schatten *et al*. 2005; Katayama *et al*. 2006), or microfilaments as in yeast (Yaffe 1999). While mitochondria translocation has been reported for different animals, and mitochondrial behavior has been studied particularly in *Xenopus* (Tourte *et al*. 1981; Wilding *et al*. 2001; Chang *et al*. 2004), little is known about mitochondrial behavior during early oogenesis in zebrafish, and no data are available on the relationship between mitochondria aggregation or distribution and the role of microtubules or microfilaments in this process. Whether mitochondria aggregated in the MC are involved in dynamic exchanges with ambient mitochondria is also unknown.

In the present study, we observed changes in mitochondrial aggregation and distribution within the cytoplasm of early zebrafish oocytes by using Mito Tracker stains and JC-1 (5,5′,6,6′-tetrachloro-1,1′,3,3′-tetraethylbenzimidazolylcarbocyanine iodide) to label mitochondria. We used microtubule and microfilament inhibitors, and methods of fluorescence recovery after photobleaching (FRAP), to determine mitochondrial behavior. We also studied mitochondria interactions between aggregated and dispersed states, and the relationship between mitochondria and the cytoskeleton.

Materials and methods

Animals and oocytes

Zebrafish were raised and maintained according to methods described by Westerfield (1995). Ovaries were removed from freshly killed females and immediately rinsed with D-PBS (Dulbecco's phosphate-buffered saline: KCl, 2.67 mM; KH_2PO_2, 1.47 mM; NaCl, 138.00 mM; Na_2HPO_4, 8.10 mM; pH 7.4), and dissected in 65% Leibovitz L-15 medium (Sigma, St. Louis, MO, USA) by repeated pipetting. Before separation of early stage I oocytes, the ovary tissue was treated with 2 mg/mL collagenase I in 65% L-15, for 30 min, and then washed twice with enzyme-free medium. Selman *et al*. (1993) had classified the zebrafish oocytes into five stages. They stated that stage I is the primary growth stage, and oocytes are transparent, with diameters from 7 to 140 μm; stage II oocytes are from 140 to 340 μm in diameter, and cortical alveolus developed in the ooplasm. In our experiments, we mainly observed stage I and early stage II oocytes. Compared with the entire oocyte development span, they are in the period of early oogenesis.

Staining of mitochondria with probes

Fresh oocytes were placed into a well of a four-well culture plate, washed twice with 65% L-15. After the medium was aspirated, 1 mL of 65% L-15 containing 500 nM Mito Tracker Red CMXRos (Molecular Probes, Eugene, OR, USA), 500 nM Mito Tracker Green FM (Molecular Probes) or 5 μM JC-1 (Cell Technology

Inc., Mountain View, CA, USA) was added to the well. Then the oocytes were incubated for 45 min at 25°C in the dark on a vibrator, with the vibrating velocity about 30 turns per min. After staining, oocytes were washed with 65% L-15 three times for 20 min each time, and then observed with a confocal microscope (ZEISS LSM 510 META, Jena, Germany).

Nocodazole and cytochalasin B treatment

Stage I oocytes, with diameters from 80 to 90 μm, were cultured in 65% L-15 with microtubule assembly inhibitor nocodazole (methyl-[5-(2-thienylcarbonyl)-1H-benzimidazol-2-yl]-carbamae; 100 μM) or the microfilament inhibitor cytochalasin B (2.5 μM) for 1 h at 25°C, and then stained with JC-1 (5 μM). The staining method was the same as described above, except that 100 μM nocodazole or 2.5 μM cytochalasin B was included in the solutions. Experiments (nocodazole treatment, cytochalasin B [CB] treatment and control) were repeated six times on different days.

FCCP treatment

Oocytes were cultured in 65% L-15 with FCCP (5 μM) for 30 min at 25°C, and then stained with JC-1 (5 μM). The staining method was the same as described above, except that 5 μM FCCP was still included in the medium. Experiments were repeated three times on different days.

Confocal microscopy of stained mitochondria and fluorescence bleaching

Specimens were observed using laser scanning confocal microscopy (ZEISS LSM 510 META) in a glass bottom culture dish (35 mm Petri dish, 10 mm Micro well; Mat Tek, Ashland, MA, USA). Line laser excitations of 488 nm and 543 nm were used for green and red fluorescence, respectively. Oocytes stained with JC-1 were observed in both green and red fluorescent channels (all of the parameters were similar except that the laser lines were different, and after FCCP treatment, the detection gain and pinhole of the red channel were both higher than normal). The bleaching and recovery protocols were programmed, and then carried out automatically. Selected areas were bleached with a 100% laser scale, and images were taken at about 4-s intervals to record the bleaching effect and fluorescence recovery speed; fluorescence changes during and after bleaching were recorded. Morphological observations were repeated at least three times for each probe. Bleaching and recovery experiments were repeated six times for each treatment (nocodazole or CB) and control.

Detection of green/red fluorescence ratios in different sublocations of JC-1 stained oocyte

Green and red images were collected simultaneously under similar detect-gains and pinholes (except for the FCCP-treated oocytes, for which the parameters in red channel were about four times higher than normal) by confocal microscopy of JC-1 stained oocytes, green and red images were merged into a new image by confocal microscopy at the same time. For each merged image, we detected green and red intensity values from the entire oocyte, MC, cluster 1, cluster 2, dispersed area 1 and dispersed area 2 (the clusters and dispersed areas were randomly chosen), with Adobe photoshop 7.0. Green/red fluorescence ratios were calculated, and statistically analyzed.

Statistics

Percentages of fluorescence recovered within 3 min after bleaching were calculated for each bleaching and recovery curve of each treatment. The percentages were then treated with arcsine transformation. Green/red fluorescence ratios were calculated from the green and red intensity value pairs detected from selected sublocations in the merged images. The mean ± SD of each group was calculated by Excel for Windows. ANOVA was applied to determine whether the differences were significant among groups. Then Student-Newman-Keuls multiple range test for pairwise comparisons was carried out. The statistical significance level was set at $P < 0.05$.

Results

Mitochondrial distribution and aggregation in early oocytes

In the early stage I oocytes (diameter about 10–40 μm) most mitochondria aggregated into cluster masses of different sizes (Fig. 1E–H); they dispersed into the entire ooplasm with higher density near the nucleus (Fig. 1H). A large mitochondrial aggregate became located to one side of the nucleus; this large aggregation is termed the mitochondrial cloud (Fig. 1A,C–F,I,K–S). It gradually translocated from the perinuclear area to the vegetative cortex and then dispersed within the vegetative cortex as the oocyte developed further into the mid-stage II. As the oocyte grew bigger (> 40 μm in diameter) more mitochondria typically aggregated around the nucleus, forming a 'necklace-like'

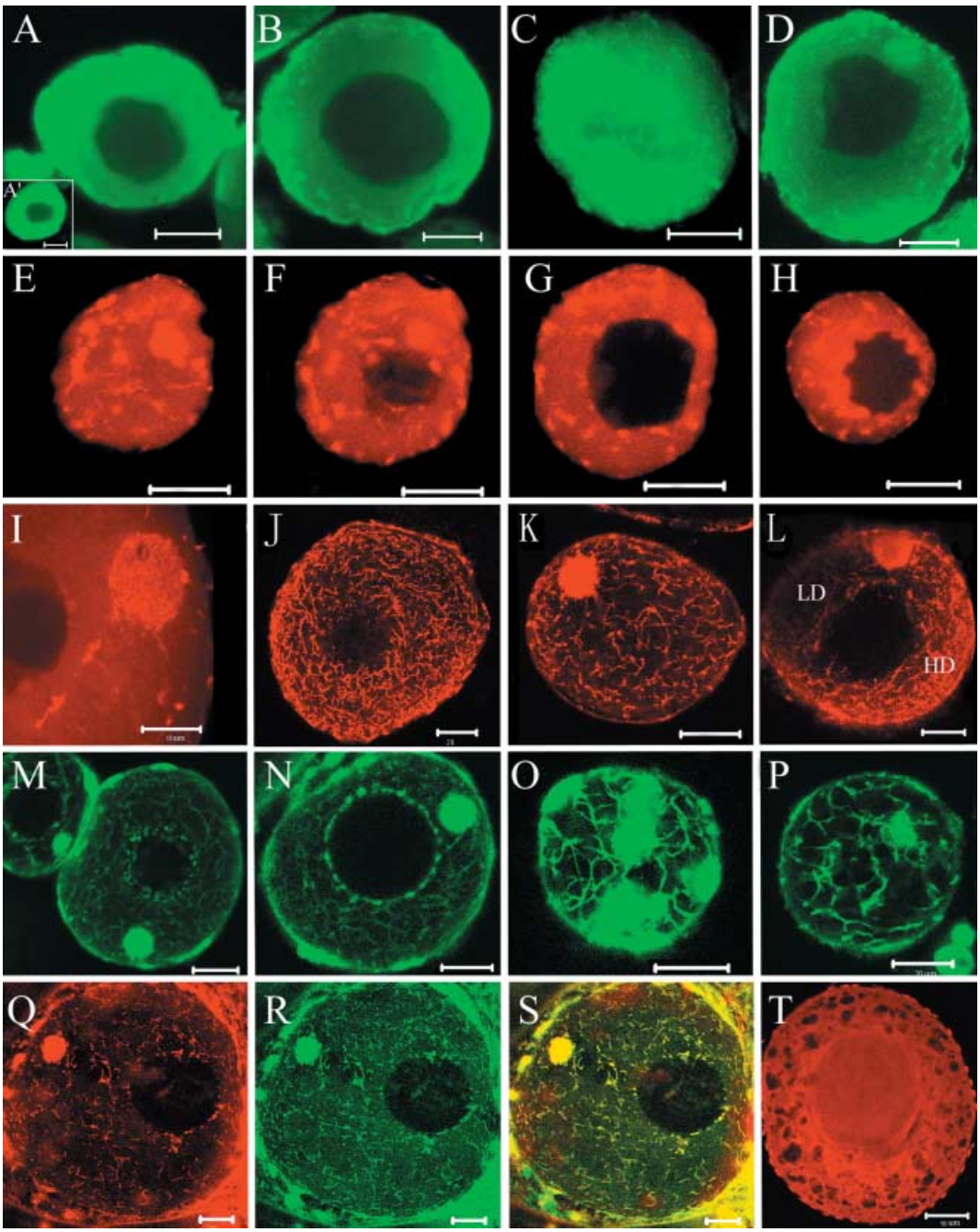

Fig. 1. Mitochondrial distribution pattern in early zebrafish oocytes, stained with Mito Tracker Green FM (A–D, and A′), Mito Tracker Red CMXRos (E–L, and T), and JC-1 (M–S). (A–D) There were usually fewer mitochondrial aggregate masses or threadlike structures in Mito Tracker Green FM stained oocytes. (A′) No mitochondrial aggregation was detected in Mito Tracker Green FM stained oocytes in sections not displaying the mitochondrial cloud (MC). (E–H) Early stage I oocyte (diameter less than 40 μm) with numerous mitochondrial aggregates in different-sized cluster masses and distribution throughout the ooplasm with higher density in the area near the nucleus. (I) A close-up of the MC. In the area outside the MC, mainly homogeneously distributed small spots are detected. This condition could be seen in a few Mito Tracker Red CMXRos or JC-1 stained oocytes. (J, K) Threadlike structures dominate the entire ooplasm in most of the mid- or late-stage I oocytes. (L) Mid- and later-stage I oocytes, a lower density mitochondrial area (LD) and a higher density mitochondrial area (HD) on the opposite sides of the germinal vesicle. (M, N) Mitochondrial aggregate masses concentrated around the nucleus. (O, P) MC connected with threadlike mitochondrial aggregations. (Q, R) The same section of an oocyte detected simultaneously in red and green channels. (S) The merged image of Q and R, showing a comparison of the distribution of mitochondria with higher or lower inner membrane potential. (T) A section of a stage II oocyte showing that only minor mitochondrial aggregation concentrated in the area around the nucleus at this stage. Generally only homogeneous small spots are distributed between the cortex vesicles. I; bar, 10 μm; T: bar, 50 μm; all other images: bar, 20 μm.

circle around the nucleus (Fig. 1M,N). The specific characteristics of mitochondria during the mid- and late-stage I zebrafish oocytes was aggregation into threadlike configurations with various lengths (Fig. 1J–S). In Mito Tracker Green FM stained oocytes, staining of these structural details was not as pronounced (Fig. 1A–D,A′), or hardly even detectable (Fig. 1A′), but in Mito Tracker Red CMXRos (Fig. 1E–L,T) and JC-1 (Fig. 1M–S) stained oocytes, structural details were very clear. The density of threadlike structures differed somewhat in different oocytes, but the configurations were similar both in Mito Tracker Red CMXRos and in JC-1 stained oocytes. Such threadlike structure disappeared in stage II oocytes (Fig. 1T). Sometimes, fewer mitochondrial aggregate masses and more areas with homogeneous tiny spots could be seen in a few Mito Tracker Red CMXRos (Fig. 1I) or JC-1 (Fig. 2E,H) stained oocytes.

The MC is a typical structure during early oogenesis in most animals studied so far. In our experiments, we noted that in early stage I zebrafish oocytes, it was connected to threadlike mitochondria aggregations

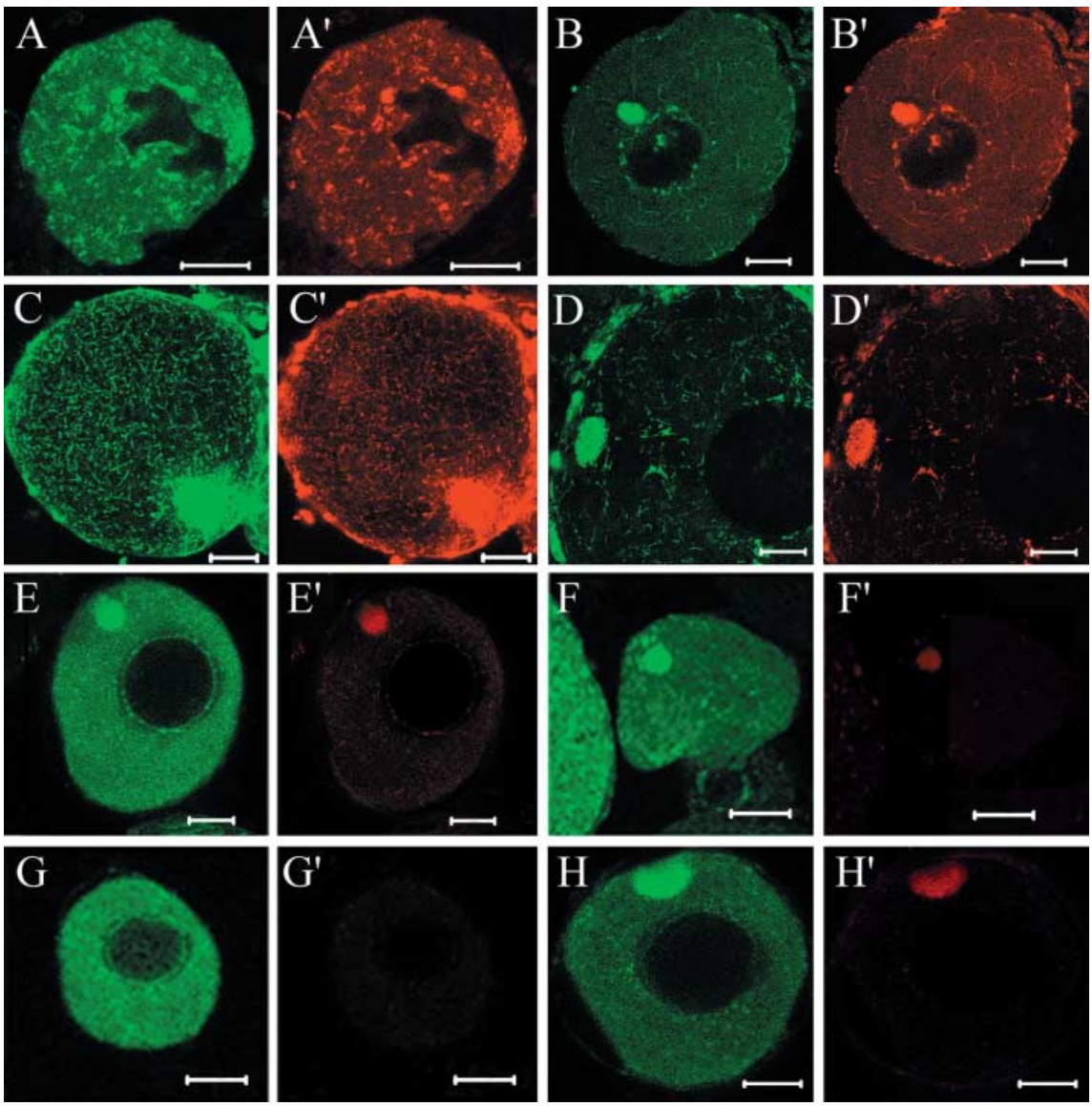

Fig. 2. Image pairs collected simultaneously in both green and red fluorescence for each section in JC-1 stained oocytes. A and A′, B and B′, and C and C′ show that the distribution of green fluorescence and red fluorescence corresponded in each observed section. D and D′ show inactive mitochondria (green fluorescence) being more dominant in the plasm. (E–H′) After FCCP treatment, the green fluorescence emission was distributed normally (E–H). In the corresponding images red fluorescence emission became very weak (E′–H′), even if the detect gain and pinhole were set about four times higher than normal. The intensity distribution at each corresponding point in the red images was similar to that in green images. Bar, 20 μm.

in a net-like organization (Fig. 1O,P). The MC appeared to be composed of threadlike and granular structures (Fig. 1I,K,O,P). In most oocytes with diameters from 40 to 70 μm, threadlike structures and other cluster masses are almost evenly distributed throughout the ooplasm, except for the MC and a denser layer around the nucleus (Fig. 1M,N). No mitochondria were found in the germinal vesicle area in the center of the cell. By analyzing sections focused every two to three microns through the entire z axes of oocytes, we detected threadlike structures distributed in the entire ooplasm (images not shown). In oocytes with diameters greater than 70 μm, aside from the MC, an area containing fewer mitochondria was detected on one side of the nucleus, which we termed the low-density area (LD, Fig. 1L). Opposite to this area across the nucleus, an area containing denser mitochondrial aggregations could be detected, which we called the high-density area (HD, Fig. 1L).

Distribution of active and inactive mitochondria

To distinguish localizations of active and inactive (low active) mitochondria in the cytoplasm of early oocytes, we used JC-1 as a mitochondrial probe, and 488 and 543 nm laser lines to excite green and red fluorescence. Active mitochondria containing JC-1 aggregates emit both red and green fluorescence, and low-active or inactive mitochondria containing dispersed JC-1 (non-aggregated), only emit green fluorescence. For each observed profile, we collected both red fluorescence (Fig. 1Q) and green fluorescence (Fig. 1R) images simultaneously from two different channels, and merged the two into one integrated image (Fig. 1S) to compare the localization of red and green signals. Table 1 shows that the red fluorescent intensity was significantly decreased in FCCP-treated oocytes, but green fluorescent intensity was not significantly changed in these oocytes (statistical data not shown). The green/red fluorescence ratios in this group were significantly higher than those of all the other groups. The green/red fluorescence ratios of MC and two cluster structures of CB- and nocodazole-treated oocytes were in the medium range (Table 1). All green/red fluorescence ratios collected from all locations of normal oocytes, dispersed areas and entire cell profiles of CB- and nocodazole-treated oocytes, were close to 1 (> 0.97 and < 1.089, Table 1). Merged images collected from normal oocytes also showed almost no difference in the distribution patterns of green and red fluorescence, whether in aggregated mitochondrial clusters or in dispersed areas (Figs 1.Q–S and 2A,A′,B,B′,C,C′), which implies that active mitochondria were distributed in all sublocations. To validate whether the red fluorescent mitochondria represented the active state, and green fluorescent mitochondria represented the inactive or low-active state, we used FCCP to uncouple mitochondrial oxidative phosphorylation. All mitochondria lost their inner membrane proton potential ($\Delta\psi$), and became 'inactive' after treatment with FCCP. After FCCP-treatment, fluorescent images showed that red fluorescence decreased to nearly undetectable levels, except for a faint red shimmer that could be detected in the MC (Fig. 2E′,F′,H′) even when the detect-gain and pinhole of the red channel was set to much higher than normal. After FCCP treatment, the green fluorescence distribution of inactive mitochondria remained unchanged similar to that in untreated oocytes (Fig. 2E–H, statistical data not shown) and the green/red fluorescence ratios that became highly significant increased (Table 1).

Table 1. Mean ± SD of green/red fluorescence ratios of sublocations in different oocyte groups stained by JC-1

Groups of oocyte	Sub-location and abbreviations	Mean ± SD	Groups of oocyte	Sub-location and abbreviations	Mean ± SD
Normal oocytes (n = 15)	Entire cell (Ne)	0.995 ± 0.284 (a)	CB treated oocytes (n = 12)	Entire cell (Ce)	1.020 ± 0.103 (a)
	MC (Nm)	1.040 ± 0.317 (a)		MC (Cm)	1.211 ± 0.156 (b)
	Cluster 1 (Nc1)	1.088 ± 0.309 (a)		Cluster 1 (Cc1)	1.315 ± 0.215 (b)
	Cluster 2 (Nc2)	1.011 ± 0.204 (a)		Cluster 2 (Cc2)	1.289 ± 0.209 (b)
	Dispersed 1 (Nd1)	1.048 ± 0.360 (a)		Dispersed 1 (Cd1)	0.994 ± 0.131 (a)
	Dispersed 2 (Nd2)	0.970 ± 0.307 (a)		Dispersed 2 (Cd2)	0.980 ± 0.099 (a)
FCCP treated oocytes (n = 13)	Entire cell (Fe)	2.565 ± 1.287 (c)	Nocodazole treated oocytes (n = 9)	Entire cell (Noe)	0.972 ± 0.275 (a)
	MC (Fm)	1.879 ± 0.954 (c)		MC (Nom)	1.080 ± 0.135 (a)
	Cluster 1 (Fc1)	3.267 ± 2.170 (c)		Cluster 1 (Noc1)	1.278 ± 0.283 (b)
	Cluster 2 (Fc2)	4.173 ± 2.919 (c)		Cluster 2 (Noc2)	1.136 ± 0.280 (b)
	Dispersed 1 (Fd1)	2.724 ± 1.426 (c)		Dispersed 1 (Nod1)	1.061 ± 0.342 (a)
	Dispersed 2 (Fd2)	2.850 ± 1.790 (c)		Dispersed 2 (Nod2)	1.048 ± 0.266 (a)

In the table, a, b, c represent different statistical significant levels.

Mitochondrial movement analysis by fluorescence recovery after photobleaching

By using the fluorescence photobleaching technique, we detected that mitochondria were in dynamic movement in early zebrafish oocytes. When fluorescence was bleached out in selected areas by a strong laser, mitochondria in the bleached area lost fluorescence. Fluorescence of JC-1 molecules could not recover in these mitochondria during our measuring period. But after mitochondria with fluorescence translocated into this bleached area from other areas, the bleached area could partially recover fluorescence. In JC-1 labeled oocytes, active and inactive mitochondria translocated almost in the same manner (Fig. 3A,A′). The results also showed that the fluorescence recovery speed was related to the location and size of the bleached area. The smaller the area, the faster the recovery speed. In the denser mitochondrial aggregate area, fluorescence recovery was fastest. Fluorescence in the MC clearly recovered faster than that in other areas (Fig. 3B,B′) after bleaching. Fluorescence in the area near the MC also recovered faster than those of more distant areas (Fig. 3C,C′). When the bleached area was larger, recovery speed became slower (Fig. 3D,D′), especially in the areas with less densely aggregated mitochondria (Fig. 3E,E′). When we bleached out all of the fluorescence in the entire profile of the cell, fluorescence could not recover (Fig. 3F,F′), which confirms that after bleaching, fluorescence of JC-1 could not recover during the measuring period. In fixed oocytes, fluorescence also could not recover in the bleached areas (images not shown). Mitochondrial clusters usually aggregate into a concentrated layer surrounding the nucleus; fluorescence recovery after bleaching was also faster in this layer compared with that in other ooplasmic areas except for the MC (Fig. 3G,G′). In Figure 3(H), we show images before bleaching (first two images) and during the recovery process after bleaching (the third image was immediately after bleaching, and the subsequent images show the recovery progress of fluorescence).

In the time-lapse images (Fig. 4), we could also observe that the cluster structures changed their shapes with time, although their positions did not move within a few minutes. This also indicates that mitochondria were moving in and out of the aggregate structures; it indicates that mitochondria in these structures are in a dynamic state.

Effects of microtubule and microfilament modulators on mitochondrial movement

Since microtubules and microfilaments typically regulate translocation of mitochondria and other organelles (Yaffe 1999; Sun *et al*. 2001; Sun & Schatten 2006), we treated oocytes with nocodazole or cytochalasin B to examine mitochondrial distribution movement after bleaching of fluorescence in different selected areas. Different than expected, we did not detect a decrease in the mitochondrial movement speed. Instead, it increased after noccodazole or CB treatment. We repeated our experiments three more times and obtained the same results. Since fluorescent recovery speed after bleaching was different in various cytoplasmic areas, we chose the entire MC in oocytes with diameters from 80 to 90 μm (in some of the given profiles the diameter may be smaller since the profile with MC may not represent the largest area of the oocyte), as the selected area for fluorescence bleaching in the control, nocodazole treated, or CB treated groups. We recorded the recovery plots and calculated percentages of fluorescence recovered in oocytes of different groups, respectively. Figure 5 shows representative results for each group (control: A and A′; CB treated: B and B′; and nocodazole treated: C and C′). The mean ± SD of their fluorescence recovery percentages were 31 ± 2.1%, 36 ± 2.3% and 43 ± 2.8%, respectively, for control, nocodazole treated and CB treated groups (Fig. 5D). In all samples studied, fluorescence never recovered to their original levels after bleaching. In the control group, fluorescence recovered in the first 2–3 min, and then slowed down and recovery ceased (Fig. 5A,A′). In CB treated oocytes, fluorescence recovered sooner and usually reached a higher level compared with control oocytes (Fig. 5B,B′). In nocodazole treated oocytes, fluorescent recovery speed and extent after bleaching were in the medium range (Fig. 5C,C′). Statistical analysis showed that the difference was significant ($P \approx 0.035$) only between the CB treated groups and control groups (Fig. 5D).

Discussion

Morphology and distribution of mitochondria during early oogenesis in zebrafish

In the present study, we report varied amounts of long threadlike mitochondrial structures in more than 60% of early zebrafish oocytes that were typically connected into a network and have not been reported for other animals so far. Since Mito Tracker and JC-1 labeling are mitochondria-selective (Poot *et al*. 1996; Wilding *et al*. 2001; Van Blerkom *et al*. 2002), we conclude that the threadlike structures and other aggregate masses stained by the three probes are indeed mitochondria. Since in most fixed specimens, mitochondria are usually seen as dispersed small

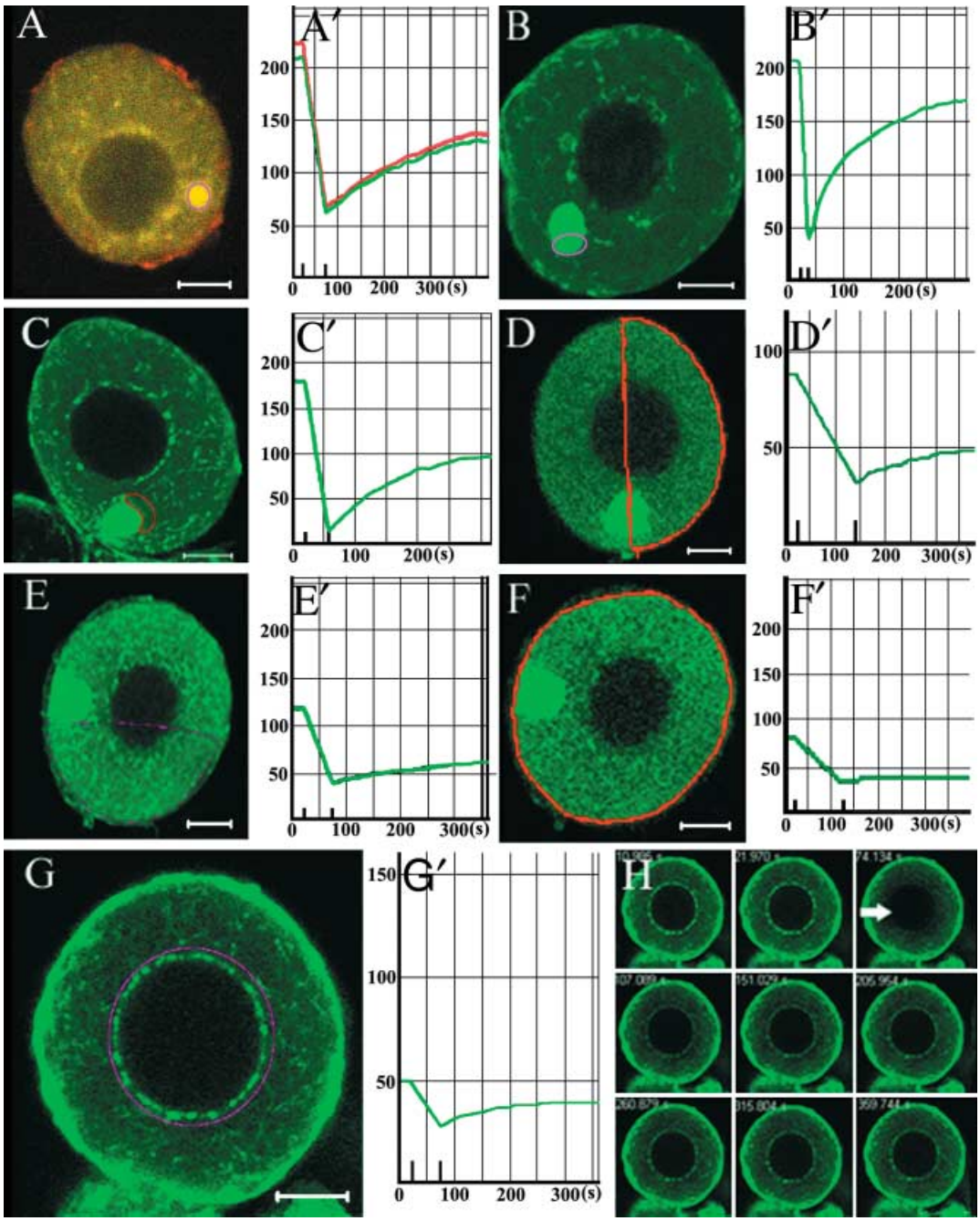

Fig. 3. Images show fluorescence bleaching and recovery results. Bleached areas are circled with red or pink lines, and the plots show the changes of fluorescent intensity occurring within the circled areas. (A and A′) Oocyte stained with JC-1 and detected simultaneously with both green and red fluorescence. The recovery speeds and extents of green and red fluorescence were similar (31 ± 4.2% recovery, $n = 5$, red). Only green fluorescence bleaching and recovery is described in the following. (B and B′) The recovery speed was faster when only part of the MC was bleached (62 ± 10.0% recovery, $n = 6$). (C and C′) Recovery speed was slower in the area near the MC compared with that in the MC (30 ± 12.5% recovery, $n = 4$). (D and D′) Half of the cell (including half of the MC) was bleached, and the recovery speed was slower (26 ± 7.7% recovery, $n = 5$). (E and E′) half of the cell (not including the MC) was bleached, and the recovery speed was further slowed (22 ± 7.4% recovery, $n = 4$). (F and F′) the entire cell was bleached, and almost no recovery was seen (1.6 ± 0.8% recovery, $n = 4$). (G and G′) Mitochondrial aggregations around the nucleus were bleached (8.4 ± 3.7% recovery included the black nuclear area; and 30 ± 6.8% recovery, not including the black nuclear area; $n = 3$, plot was not shown). (H [same oocyte as G]) Fluorescence recovery of mitochondrial aggregations around the nucleus. The first two images are before bleaching, the third immediately after bleaching (arrow points at the bleached area), and all of the latter images show the recovery process. Statistically significant grades: B was in grade a; A, C and G (not including black nuclear area) were in grade b; D was in grade c; E was in grade d; F was in grade e.

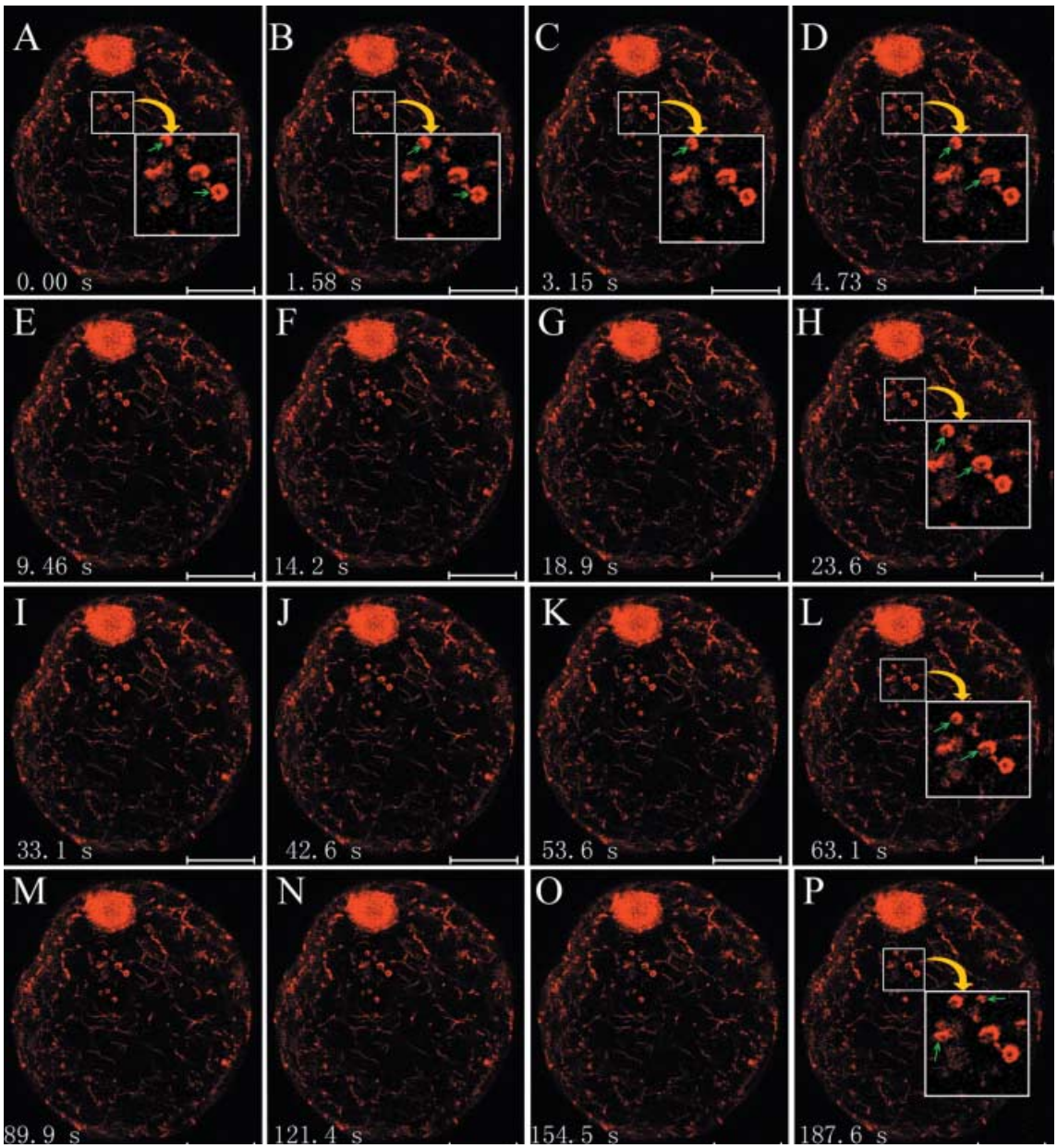

Fig. 4. Time-lapse images show that the mitochondrial aggregate structures are changing in shapes with elapsed time, which implies that mitochondria are moving in and out of the aggregate structures, with the outgoing and incoming speeds not matching at each point, so the shape of the structure changed. In some images, a chosen area was magnified; green arrows indicate that structural shapes obviously changed compared with those in images before or after. Bar, 20 μm.

clusters or homogeneous small spots, we suggest that fixation or other harsh preparation procedures could cause breakage of the long threadlike mitochondria into smaller structures, which may explain why we mostly see short threads or small structures of mitochondria in fixed specimens, especially when analyzed with transmission electron microscopy. Mito Tracker Green FM staining differed from Mito Tracker Red CMXRos or JC-1 labeling in that it stained fewer threadlike structures; Mito Tracker Green FM may be more toxic to the oocyte or mitochondria than the latter two probes. The threadlike structures are different in diameters (Fig. 1J–S) and stained almost equal in green and red intensity values (Table 1; Fig. 1.Q,R and 2A, A′,B,B′,C,C′,D,D′), they may be composed of different individual mitochondria. The general pattern of mitochondrial distribution and aggregation during early oogenesis in zebrafish is similar to that reported in other animals, and very similar to that in *Xenopus* (Schnapp *et al.* 1997; Wilding *et al.* 2001; Chang

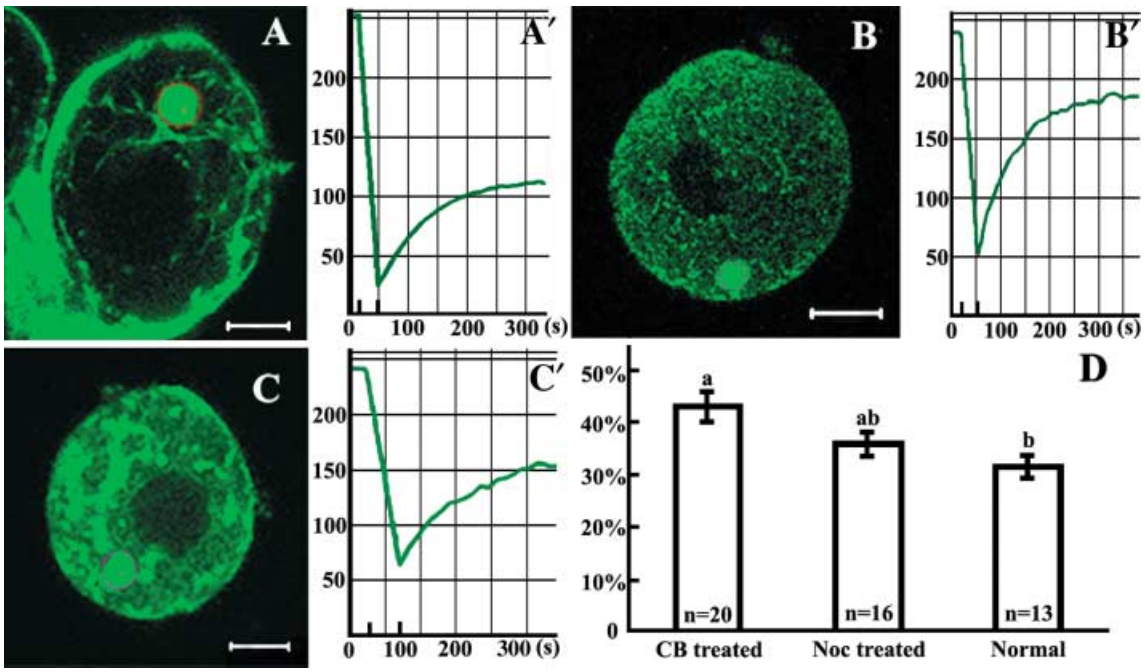

Fig. 5. Fluorescence recovery speeds and extents in the MC in control, cytochalasin B and nocodazole treated oocytes after bleaching. (A and A′) show the recovery speed and extent in control oocytes. (B and B′) show that the recovery speed was fastest and the extent was highest in cytochalasin B treated oocytes. (C and C′) show that in nocodazole treated oocytes, the recovery speed was faster than that in control oocytes, but slower than that in cytochalasin B treated Oocytes. The extent of recovery was also higher than that in control oocytes, but lower than that in cytochalasin B treated oocytes. (D) The percentages of recovered fluorescent density in all groups are shown as columns. Total numbers of oocytes detected in the separately repeated experiments are shown as *n*. Significant difference was found only between cytochalasin B treatment and control groups ($P \approx 0.035$). Different letters (a or b) show that their difference is significant.

et al. 2004). In both species, mitochondria first randomly aggregated in small groups throughout the cytoplasm, being more concentrated near the nucleus; then more of the aggregated mitochondrial clusters become closely located around the nucleus, and formed a 'necklace-like' circle in profile (Gondos *et al*. 1986; Jansen & de Boer 1998). Some of the other mitochondrial clusters fuse into one bigger aggregate (the MC) on one side of the nucleus in stage I oocytes. The MC gradually translocated from the perinuclear area to the cortex of the vegetal pole, and then dispersed throughout the vegetal pole. In the present study we found that the MC, especially in the early phase of its formation, was connected to numerous ramified long threadlike mitochondria radiating from the MC. Molecular communication may exist between the MC and other mitochondria in surrounding areas.

In this paper we report polar distribution of mitochondria in zebrafish oocytes. In the vegetal pole area, mitochondria became sparse, and the MC was always located at one side of this area. In the cytoplasm of the animal pole area, mitochondria became densely distributed. Such distribution may represent differences in energy requirements at the two poles. Though we first noticed such distribution in oocytes with diameters of about 70 μm, we believe that it may be a gradual progress. This mitochondrial distribution pattern has not been observed in other animals as reported so far.

Kloc *et al*. (1996) showed that the transport of the Xlsirt RNA from its site of synthesis to the MC is microtubule- and microfilament-independent. It remains unclear how the RNA is translocated into the MC, and whether the MC attracts them, or whether they attract mitochondria to aggregate into the MC. Chang *et al*. (2004) reported that the germ plasm RNAs were entrapped into the MC. There are also reports about the 3′-untranslated region (3′UTR) of some RNAs in germ plasm, such as the Xcat2 3′UTR possessing a mitochondrial cloud localization element (MCLE) and a germinal granule localization element (GGLE) (Zhou & King 1996; Kloc *et al*. 2000; Kosaka *et al*. 2007). Kosaka *et al*. (2007) found that the RNA-binding protein, Hermes, originally found in *Xenopus*, is a component of MC in zebrafish, too. We propose that the mitochondria are attracted by some proteins or/and RNAs to aggregate into the MC, but whether

it is for energy supply alone or also for other purposes remains unclear. Mitochondria also aggregated in other areas in addition to the MC, and this may be the result of small amounts of related proteins and/or RNAs localized in these areas that attract mitochondria to aggregate.

Distribution of active and inactive mitochondria

It has been reported that active and inactive mitochondria may distribute differently, each having their domains, during early oogenesis in human and other animals (Wilding *et al*. 2001; Van Blerkom *et al*. 2002), but we did not find such difference during early oogenesis in zebrafish. In our JC-1 stained oocytes, by merging the red fluorescence image (Fig. 1Q) and green fluorescence image (Fig. 1R) collected simultaneously from the same profile, we found that all of the cluster structures became orange in color and there were few areas left with only green or red color (Fig. 1S). By detecting and calculating green/red fluorescence ratios of cluster structures, MC, dispersed areas and entire cell profiles, we found that the ratios of all of these locations in normal oocytes were close to 1 (no statistical difference), which means that green and red fluorescence intensity were almost the same in all of these locations. Since no green area alone was found, we conclude that the inactive mitochondria (emission of green fluorescence only) domain may not exist. Just based on the phenomenon of that green and red fluorescence intensities corresponded to each other in all sublocations (Table 1), we still cannot say inactive and active mitochondria are always colocalized, because active mitochondria emit green fluorescence as well as red fluorescence. However, if inactive mitochondria do exist above the negligible level, they would be colocalized with the active mitochondria, otherwise the green/red ratios would vary in different locations. In FCCP-treated oocytes, the red fluorescent intensity significantly decreased in all clusters and dispersed areas; the green/red ratios were all changed into a much higher level (no statistical significant difference, Table 1). CB- and nocodazole-treatment significantly decreased red fluorescent intensity in cluster structures and MC, but not in the dispersed areas (Table 1) and the reason for this is still unclear. It may relate to the increases of mitochondrial free movement in these oocytes. Since after treatment with FCCP, active (red fluorescent) mitochondria almost all disappeared and red fluorescence decreased significantly, it is implied that the red fluorescence was emitted from active mitochondria in untreated specimens. The red shimmer remaining after FCCP treatment in the MC, might indicate a few remaining active mitochondria that were not affected or only partly affected by FCCP, since mitochondria were too dense in this area, and FCCP may not have reached all of them. It is also possible that the characteristics of mitochondria in this area are somewhat different from that of mitochondria in other areas.

Mitochondrial movement in the cytoplasm of early oocytes

The recovery speed of fluorescence after photobleaching proved that mitochondria are in dynamic movement in early zebrafish oocytes. Since in the smaller bleached area, the distance is shorter for mitochondria to distribute, fluorescence recovery is faster. In Figure 3(D,D′), recovery speed is faster than that in E and E′. Since in the former oocyte, the bleached area included half of the MC, more mitochondria can easily distribute to the bleached area from the other half of the MC (which was not bleached). However, in oocytes like those shown in Figure 3(E,E′), where the bleached area does not include the MC or other obvious mitochondrial aggregations, the fluorescence recovery speed was slower. This also showed that mitochondria in the MC could be freely moving, even moving out of the MC, and mitochondria from nearby areas can also move into the MC. This indicates that the MC is not a separate area for only a specific kind of mitochondria. The cluster masses around the nucleus are also not a separate entity. In these cluster masses, including the MC, some molecular activities, such as mtDNA replication, or perhaps repair or recombination, or mtrRNAs moving out, may be faster or slower as some authors have suggested (Mignotte *et al*. 1987; Kobayashi *et al*. 1993; Kashikawa *et al*. 2001; Snee & Macdonald 2004; Amikura *et al*. 2005; Cao *et al*. 2007). The aggregate cluster masses may have specific functions. We detected that the shapes of aggregated mitochondrial clusters are changing in time lapse studies (Fig. 4), which also implies that some mitochondria in these structures are moving out of the structure, while other mitochondria are moving into it. As the speed of incoming and outgoing mitochondria at each point of the clusters is not equal, the structural shapes would slightly change with time. When fluorescence was totally bleached out from the entire profile of the cell, fluorescence could not recover, since no mitochondria with fluorescence were left to move into the bleached area (Fig. 3F,F′). In fixed oocytes, mitochondria are prevented from translocation since proteins in the cytoplasm are all denatured and immobilized.

Role of microtubules and microfilaments in mitochondrial distribution

It is well established that both microtubules and microfilaments play an important role in regulating mitochondria and other organelle movements (Yaffe 1999; Sun *et al*. 2001; Schatten *et al*. 2005) although they may not always regulate movement of all mitochondria at a given time. Nocodazole and CB have been widely used in many cell types, including mammalian cells, sea urchin and *Xenopus* oocytes and eggs, in different doses from 0.33 nM to 100 μM, and treatment times from 15 min to 16 h (Janicot & Lane 1989; Van Blerkom 1991; Salman *et al*. 2001; Strickland *et al*. 2005; Katayama *et al*. 2006; Sun & Schatten 2006) to depolymerize microtubules and microfilaments. In our experiments, after treatment with nocodazole or CB, mitochondrial free movement speed increased slightly (in nocodazole treated oocytes) or significantly (in CB treated oocytes). We conclude that after depolymerizing microtubules and microfilaments, mitochondria movement may become uninhibited. Under physiological conditions mitochondria may be anchored to microtubules and/or microfilaments to allow controlled and directed movement. Mitochondrial free movement became faster after CB treatment than after nocodazole treatment, which may imply that more mitochondria are anchored to microfilaments than microtubules, or microfilaments may hold mitochondria more tightly than microtubules. The fact that CB- and nocodazole-treatment significantly reduced the red fluorescent intensities in clusters and MC, but not in the dispersed areas (Table 1), may also be related to the increase of mitochodnrial free movement.

We noted that mitochondrial localization was not the same in all the zebrafish oocytes; a small percentage of oocytes contained mitochondria that were not distributed in accordance with the general rule, which may represent differences in oocyte quality.

Acknowledgments

The authors appreciate Ms. Shiwen Li, Hua Qin, Xiaoqiu Liu & Mr Yabing Liu for their assistance with confocal microscopy. This study was supported by grants from the Ministry of Sciences and Technology of China (2006CB944001 & 2006CB504004); the National Natural Science Foundation of China (30430530); the Chinese Academy of Sciences (KSCX2-YW-R-52); and the Chinese Post-doctoral Association 20050038391.

References

Amikura, R., Hanyu, K., Kashikawa, M. & Kobayashi, S. 2001. Tudor protein is essential for the localization of mitochondrial RNAs in polar granules of *Drosophila* embryos. *Mech. Dev*. **107**, 97–104.

Amikura, R., Sato, K. & Kobayashi, S. 2005. Role of mitochondrial ribosome-dependent translation in germline formation in *Drosophila* embryos. *Mech. Dev*. **122**, 1087–1093.

Barritt, J., Brenner, C., Cohen, J. & Matt, D. 1999. Mitochondrial rearrangements in human oocytes and embryos. *Mol. Hum. Reprod*. **5**, 927–933.

Barritt, J. A., Kokot, M., Cohen, J. *et al*. 2002. Quantification of human ooplamic mitochondria. *Reprod. Biomed*. **4**, 243–247.

Bergstrom, C. T. & Pritchard, J. 1998. Germline bottlenecks and the evolutionary maintenance of mitochondrial genomes. *Genet*. **149**, 2135–2146.

Biliñski, S. M., Jaglarz, M. K., Szymanska, B. *et al*. 2004. Sm proteins, the constituents of the spliceosome, are components of nuage and mitochondrial cement in *Xenopus* oocytes. *Exp. Cell. Res*. **299**, 171–178.

Cao, L., Shitara, H., Horii, T. *et al*. 2007. The mitochondrial bottleneck occurs without reduction of mtDNA content in female mouse germ cells. *Nat. Genet*. **39**, 386–390.

Chang, P., Torres, J., Lewis, R. A. *et al*. 2004. Location of RNAs to the mitochondrial cloud in *Xenopus* oocytes through entrapment and association with endoplasmic reticulum. *Mol. Biol. Cell*. **15**, 4669–4681.

Ding, D., Parkhurst, S. M., Halsell, S. R. & Lipshitz, H. D. 1993. Dynamic hsp83 RNA localization during *Drosophila* oogenesis and embryogenesis. *Mol. Cell. Biol*. **13**, 3773–3781.

Dumollard, R., Duchen, M. & Duchen, J. 2007. The role of mitochondrial function in the oocyte and embryo. *Cur. Top. Dev. Biol*. **77**, 21–49.

Forristall, C., Pondel, M., Chen, L. & King, M. L. 1995. Patterns of localisation and cytoskeletal association of two vegetally localized RNAs, Vg1 and Xcat-2. *Development* **121**, 201–208.

Gondos, B., Westergaard, L. & Byskov, A. G. 1986. Initiation of oogenesis in the human fetal ovary: ultrastructural and squash preparation study. *Am. J. Obstet. Gynecol*. **155**, 189–195.

Iida. T. & Kobayashi, S. 1998. Essential role of mitochondrially encoded large rRNA for germ-line formation in *Drosophila* embryos. *PNAS* **95**, 11274–11278.

Janicot, M. & Lane, M. D. 1989. Activation of glucose uptake by insulin and insulin-like growth factor I in Xenopus oocyte. *PNAS* **86**, 2642–2646.

Jansen, R. P. & de Boer, K. 1998. The bottleneck: mitochondrial imperatives in oogenesis and ovarian follicular fate. *Mol. Cell. Endocrinol*. **145**, 81–88.

Karbowski, M., Spodnik, J. H., Teranishi, M. *et al*. 2000. Opposite effects of microtubule-stabilizing and microtubule-destabilizing drugs on biogenesis of mitochondria in mammalian cells. *J. Cell Sci*. **114**, 281–291.

Kashikawa, M., Amikura, R. & Kobayashi, S. 2001. Mitochondrial small ribosomal RNA is a component of germinal granules in *Xenopus* embryos. *Mech. Dev*. **101**, 71–77.

Katayama, M., Zhong, Z., Lai, L. *et al*. 2006. Mitochondrial distribution and microtubule organization in fertilized and cloned porcine embryos: implications for developmental potential. *Dev. Biol*. **299**, 206–220.

Kloc, M., Biliński, S., Chan, P. Y. & Etkin, L. D. 2000. The targeting of Xcat2 mRNA to the germinal granules depends on a cis-acting germinal granule localization element within the 3′UTR. *Dev. Biol*. **217**, 221–229.

Kloc, M. & Etkin, L. D. 1994. Delocalization of Vg1 mRNA from the vegetal cortex in *Xenopus* oocytes after destruction of Xlsirt RNA. *Science* **265**, 1101–1103.

Kloc, M. & Etkin, L. D. 1995. Two distinct pathways for the localization of RNAs at the vegetal cortex in *Xenopus* oocytes. *Development* **121**, 287–297.

Kloc, M. & Etkin, L. D. 1998. Apparent continuity between the messenger transport organizer and late RNA localization pathways during oogenesis in *Xenopus*. *Mech. Dev*. **73**, 95–106.

Kloc, M., Spohr, G. & Etkin, L. D. 1993. Translocation of Repetitive RNA sequences with the germ plasm in *Xenopus* oocytes. *Science* **262**, 1712–1714.

Kloc, M., Larabell, C. & Etkin, L. D. 1996. Elaboration of the messenger transport organizer pathway for localization of RNA to the vegetal cortex of *Xenopus* oocytes. *Dev. Biol*. **180**, 119–130.

Knaut, H., Pelegri, F., Bohmann, K. *et al*. 2000. Zebrafish vasa RNA but not its protein is a component of the germ plasm and segregates asymmetrically before germline specification. *J. Cell Biol*. **149**, 875–888.

Kobayashi, S., Amikura, R. & Mukai, M. 1998. Localization of mitochondrial large ribosomal RNA in germ plasm of *Xenopus* embryos. *Curr. Biol*. **8**, 1117–1120.

Kobayashi, S., Amikura, R. & Okada, M. 1993. Presence of mitochondrial large ribosomal RNA outside mitochondria in germ plasm of *Drosophila* melanogaster. *Science* **260**, 1521–1524.

Kobayashi, S. & Okada, M. 1989. Restoration of pole-cell-forming ability to u.v. irradiated *Drosophila* embryos by injection of mitochondrial lrRNA. *Development* **107**, 733–742.

Kosaka, K., Kawakami, K., Sakamoto, H. & Inoue, K. 2007. Spatiotemporal localization of germ plasm RNAs during zebrafish oogenesis. *Mech. Dev*. **124**, 279–289.

Marchington, D. R., Macaulay, V., Hartshorne, G. M. *et al*. 1998. Evidence from human oocytes for a genetic bottleneck in an mtDNA disease. *Am. J. Hum. Genet*. **63**, 769–775.

Mignotte, F., Tourte, M. & Mounolou, J. C. 1987. Segregation of mitochondria in the cytoplasm of Xenopus Vitellogenic oocytes. *Biol. Cell* **60**, 97–102.

Nishi, Y., Takeshita, T., Stato, K. & Araki, T. 2003. Change of the Mitochondrial Distribution in Mouse Ooplasm during *In Vitro* Maturation. *J. Nippon Med. Sch*. **70**, 408–415.

Pakendorf, B. & Stoneking, M. 2005. Mitochondrial DNA and human evolution. *Ann. Rev. Genom. Hum. Genet*. **6**, 165–183.

Perez, G. I., Trbovich, A. M., Gosgen, R. G. & Tilly, J. L. 2000. Mitochondria and the death of oocytes. *Nature* **403**, 500.

Poot, M., Zhang, Y. Z., Krämer, J. A. *et al*. 1996. Analysis of mitochondrial morphology and function with novel fixable fluorescent stains. *J. Histochem. Cytochem*. **44**, 1363–1372.

Reunov, A., Isaeva, V., Au, D. & Wu, R. 2000. Nuage constituents arising from mitochondria: is it possible? *Dev. Growth Differ*. **42**, 139–143.

Reynier, P., Chrétien, M. F., Savagner. F. *et al*. 1998. Long PCR analysis of human gamete mtDNA suggests defective mitochondrial maintenance in spermatozoa and support the bottleneck theory for oocytes. *Bioch. Bioph. Res. Com*. **252**, 373–377.

Saccone, C., Gissi, C., Reyes, A. *et al*. 2002. Mitochondrial DNA in metazoan: degree of freedom in a frozen event. *Gene* **286**, 3–12.

Salman, H., Zbaida, D., Rabin, Y. *et al*. 2001. Kinetics and mechanism of DNA uptake into the cell nucleus. *PNAS* **98**, 7247–7252.

Schatten, H., Prather, R. S. & Sun, Q. Y. 2005. The significance of mitochondria for embryo development in cloned farm animals. *Mitochondrion* **5**, 303–321.

Schnapp, B. J., Arn, E. A., Deshler, J. O. & Highet, M. I. 1997. RNA localization in *Xenopus* oocytes. *Semiar Cell. Dev. Biol*. **8**, 529–540.

Selman, K., Wallace, R. A., Sarka, A. & Qi, X. P. 1993. Stages of oocyte development in the Zebrafish *Brachydanio rerio*. *J. Morph*. **218**, 203–224.

Snee, M. J. & Machdonald, P. M. 2004. Live imaging of nuage and polar granules: evidence against a preursor-product relationship and a novel role for Oskar in stabilization of polar granule components. *J. Cell Sci*. **117**, 2109–2120.

Strickland, L. I., Donnelly, E. J. & Burgess, D. R. 2005. Induction of cytokinesis is independent of precisely regulated microtubule dynamics. *Mol. Biol. Cell* **16**, 4485–4494.

Suganuma, N., Kitagawa, T., Nawa, A. & Tomoda, Y. 1993. Human ovarian aging and mitochondrial DNA deletion. *Horm. Res*. **39** (Suppl. 1), 16–21.

Sun, Q. Y. & Schatten, H. 2006. Regulation of dynamic events by microfilaments during oocyte maturation and fertilization. *Reproduction* **131**, 193–205.

Sun, Q. Y., Wu, G. M., Lai, L. X. *et al*. 2001. Translocation of active mitochondria during oocyte maturation, fertilization and early embryo development *in vitro*. *Reproduction* **122**, 155–163.

Torner, H., Brüssow, K. P., Alm, H. *et al*. 2004. Mitochondrial aggregation patterns and activity in porcine oocytes and apoptosis in surrounding cumulus cells depends on the stage of pre-ovulatory maturation. *Theriogenology* **61**, 1675–1689.

Tourte, M., Mignotte, F. & Mounolou, J. C. 1981. Organization and replication activity of the mitochondrial mass of oogonia and previtellogenic oocytes in *Xenopus* laevis. *Deve. Grow. Differ*. **23**, 9–21.

Van Blerkom, J. 1991. Microtubule mediation of cytoplasmic and nuclear maturation during the early stages of resumed meiosis in cultured mose oocytes. *PNAS* **88**, 5031–5035.

Van Blerkom, J., Davis, P., Mathwig, V. & Alexander, S. 2002. Domains of high-polarized mitochondria may occur in mouse and human oocytes and early embryos. *Hum. Reprod*. **17**, 393–406.

Wallace, D. C., Shoffner, J. M., Trounce, I. *et al*. 1995. Mitochondrial DNA mutations in human degenerative diseases and aging. *Biochim. Biophys. Acta* **1271**, 141–151.

Wallace, D. C., Singh, G., Lott, M. T. *et al*. 1988. Mitochondrial DNA mutation associated with Leber's hereditary optic neuropathy. *Science* **242**, 1427–1430.

Webster, B. L., Mackenzie-Dodds, J. A., Telford, M. J. & Littlewood, T. J. 2007. The mitochondrial genome of Priapulus caudatus Lamarck (Priapulida: Priapulidae). *Gene* **389**, 96–105.

Westerfield, M. 1995. *The Zebrafish Book: a Guide for the Laboratory Use of Zebrafish (Brachydanio Rerio)*, pp. 1.1–1.10. University of Oregon Press, Eugene.

Wilding, M., Carotenuto, R., Infante, V. *et al*. 2001a. Confocal microscopy analysis of the activity of mitochondria contained within the 'mitochondrial cloud' during oogenesis in *Xenopus* laevis. *Zygote* **9**, 347–352.

Wilding, M., Dale, B., Marino, M. *et al*. 2001b. Mitochondrial aggregation patterns and activity in human oocytes and preimplantation embryos. *Hum. Reprod*. **16**, 909–917.

Yaffe, M. P. 1999. The machinery of mitochondrial inheritance and behavior. *Science* **283**, 1493–1497.

Zhou, Y. & King, M. L. 1996. Localization of Xcat-2 RNA, a putative germ plasm component, to the mitochondrial cloud in *Xenopus* stage I oocytes. *Development* **122**, 2947–2953.